

Wide-Field-of-Regard Pointing, Acquisition and Tracking-System for small Laser Communication Terminals

Christopher Schmidt

Institute for Communication and Navigation
German Aerospace Center (DLR)
D-82234 Wessling, Germany
christopher.schmidt@dlr.de

Joachim Horwath

Institute for Communication and Navigation
German Aerospace Center (DLR)
D-82234 Wessling, Germany
joachim.horwath@dlr.de

Abstract— Pointing, Acquisition and Tracking (PAT)-systems are one of the central parts of a Laser Communication Terminal. In Laser Communication Terminals a staggered PAT-system consisting of Coarse Pointing Assembly (CPA) and Fine Pointing Assembly (FPA) is common. The CPA provides a Wide-Field-of-Regard (FoR) and the FPA a precise and fast alignment of the beam to the communication partner. The disadvantage is the mechanical complexity. This paper presents the development challenges of a Wide-Field-of-Regard PAT-system for small Laser Communication Terminals by combining and miniaturizing the functionality of the CPA and FPA to a single actuator.

To get a small and lightweight Wide-Field-of-Regard PAT-system, the number of moving parts has to be minimized. Therefore, the system consists of an optical setup that provides a large Field-of-View (FoV) and one single mirror actuator for beam steering – thus, CPA and FPA can be combined in just one moving component. The actuator is controlled by a Digital Signal Processor (DSP). The tracking sensor is a 4-Quadrants-Detector (4QD). During the acquisition mode, the actuator moves in a predefined scan pattern until a signal can be detected on the 4QD. Consequently, the system changes to tracking mode.

Our design approach succeeded in a FoR of more than 45° without a traditional CPA. The scan time for the complete FoR is less than 1 second. The block diagram and measurements taken with the prototype in the laboratory will be presented in this paper.

I. INTRODUCTION

Due to the limitations of microwave technology, Free-Space Optical Communication (FSO) is about to become an essential technology for the transmission of large data volume between all kinds of aerial vehicles and ground stations for applications like broadband communications [8] and remote sensing [2]. Therefore, Laser Communication Terminals with agile Pointing, Acquisition and Tracking (PAT)-systems are needed. These systems operate in three phases: in the pointing phase, the terminal performs a scan in the whole Field-of-Regard (FoR) until the communication partner has been located – this is called acquisition. The second mode is the tracking phase, where either two communication beams or one

communication and one beacon beam are kept in a closed tracking loop to achieve the proper angular orientation [1].

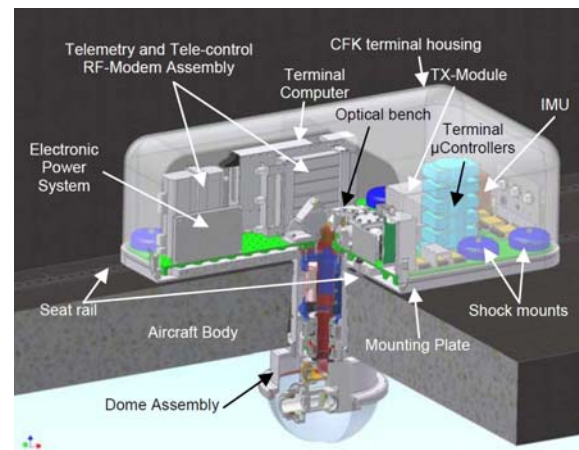


Figure 1: Free space experimental laser Terminal (FELT) for airplane-to-ground links [2]

The Optical Communication Group at the German Aerospace Center (DLR) developed a laser terminal for the use on aircrafts. Figure 1 shows the drawing of the laser terminal. This terminal has been installed in a Dornier Do 228 airplane for data transmission up to distances of several 100 km. During the pointing phase of this terminal the mechanical Coarse Pointing Assembly (CPA) is active only. The CPA is mounted under the aircraft body and covered by a dome assembly to keep away the airstream and resist weather influences. The Fine Pointing Assembly (FPA) is responsible for precise alignment of the communication partners and the compensation of vibration in the tracking mode caused by the turboprop engines of the airplane. The FPA is placed on the optical bench. The FPA actuator is a Fast Steering Mirror (FSM). Besides these parts, there is a terminal control computer and an Inertial Measurement Unit (IMU) for measuring the position and heading of the terminal. Due to the setup with a separated CPA and FPA, there is an increased mechanical complexity, system size and weight [2, 3].

New developments in the field of unmanned Micor Aerial Vehicles (MAV) enable new possibilities for FSO. These MAVs are powerful enough to carry high resolution camera systems and other sensors. The bottleneck is the real-time transmission of the high data volumes to other MAVs or to a ground station. Therefore, a new category of laser terminals is required: Small Laser Terminals (SLT) with advancements in costs, size and weight for shorter communication distances up to a few kilometers, mounted for example on a quadcopter.

To achieve these advancements, a new Pointing, Acquisition and Tracking (PAT) concept with a reduced number of moving parts and overall mechanical system complexity is needed. In this paper, the use of a combined CPA and FPA with just one single actuator as well as an advanced optical system will be shown. Chapter two describes the system design with a block diagram. In chapter three, the resulting link budget is mentioned. Chapter four explains the details of the software used for controlling the system. At the end, chapter five shows the measurements with the laboratory prototype. In chapter six, the results are summed up and chapter seven gives an outlook for future development.

II. SYSTEM DESIGN

The basic concept to reduce size and weight of the SLT is to reduce the number of moving parts and mechanical complexity. Our concept is to combine CPA and FPA in a single actuator. This principle is shown in figure 2.

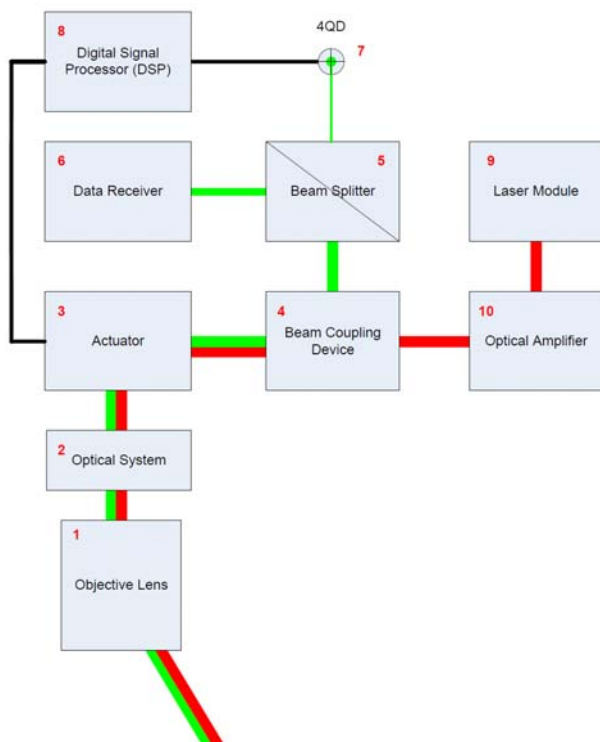


Figure 2: Basic block diagram of SLT [4]

The system consists of an objective lens (1) with a successive optical system (2), which is made of standard lenses

and adapts the diameter of the incoming (green) and outgoing (red) laser beam to the inner beam diameter of the system. The actuator (3) is the only moving part in the whole system and combines the behavior of a CPA and FPA. The beam coupling device (4) is responsible for the separation of incoming and outgoing laser beams. The outgoing laser beam is produced by a laser module (9) and amplified by an optical amplifier (10). The received laser signal is split (5) between a data receiver (6) and a 4-Quadrant-Detector (4QD) (7), which is used as a sensor for the digital signal processor (8) that controls the actuator. To reduce the costs of the SLT, it was taken care that just commercially available components have been used.

The objective lens is used as receive and transmit aperture and has to be designed for a wide Field-of-View (FoV) due to the missing mechanical CPA. The objective lens has to combine a low weight and small overall size for a high optical quality to ensure a constantly good control signal on the 4QD and on the data receiver in the whole FoV. Figure 3 shows the spot diagram for incoming beam angles of 0, 15, 20 and 28° from the optical axis of the used objective lens.

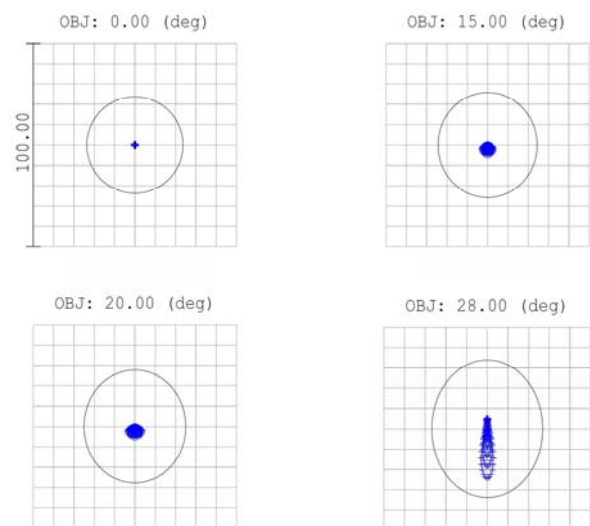


Figure 3: Spot diagram of objective lens for angles of 0, 15, 20 and 28° from the optical axis on focal plane (ZEMAX simulation), (Wavelength: 1550 nm, Unit: μm) [4]

Commercial objective lenses for photography purposes provide a high optical quality for visible light in a large FoV but come with the disadvantage of size and weight. This is due to correction lenses that are needed to avoid chromatic aberrations in the whole visible spectrum. The coating of the lenses of commercial photography objective lenses is also adapted to the visible light and causes high attenuation for wavelength in the Near Infrared (NIR). Thus, the used objective lens is typically used for industrial applications like quality conformance tests and therefore optimized for NIR-wavelengths. Due to this narrow band at a wavelength of 1550 nm, the number of correction lenses is minimized and thereby also size, cost and weight is reduced. The spot diagram shows a degradation of the spot quality for angles of $\pm 28^\circ$ and more, thus, only a FoV of $\pm 25^\circ$ will be used in the SLT.

Traditional (linear) optics suffer from a tradeoff between view angle, effective beam diameter and the overall size. For further improvement of the optical system, the use of gradient-index (GRIN) lenses as shown in figure 4 is a solution. GRIN lenses provide the advantage of a plane first surface, low aberrations, a view angle ϑ of $\pm 30^\circ$ and a paraxial magnification M , with $M=y_i/y_0$. The GRIN lenses can be directly combined with prisms and beam splitters but come with the disadvantage of a limited diameter d of momentarily 2 mm due to the production process [5].

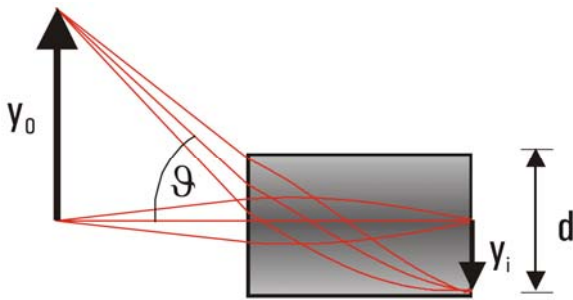


Figure 4: Schematic drawing of a gradient-index (GRIN) lens [5]

The actuator in the system is a Fast Steering Mirror (FSM) that has to fulfill the following boundary conditions: a high resolution of less than 1 μ rad, a mirror diameter larger than 10 mm, a tilt angle of more than 50 mrad and a resonant frequency of at least 1 kHz. With these conditions, the FSM is able to perform a fast and precise scan with a minimized pointing error due to the high resolution.

III. LINK BUDGET

The link budget describes the quality of a communication link and considers all gains and losses in the channel between transmitter and receiver. In this scenario, we calculate the link budget for a symmetrical scenario, which means two SLTs communicate with each other. Hence, there are the following parameters for the calculation:

- wavelength: 1550 nm
- communication distance: max. 3 km
- transmission power: max. 38 mW
- effective aperture diameter: 3.0 mm
- bit error rate: $1 \cdot 10^{-6}$

The communication scenario is defined for a wavelength in the NIR and distances up to 3 km. Due to the scenario on MAVs that are close to people, the transmission power must be at most 38 mW to achieve eye-safety. The beam diameter is given by the optical system design and used objective lenses. The link budget calculation takes also clear-sky attenuation and background light into account. With these parameters, the link margin equates 1.6 dB [4].

IV. SOFTWARE

To control the SLT, a Digital Signal Processor (DSP) is used. The DSP controls the FSM and enables all functionalities of a PAT-system: pointing, acquisition and tracking. The process chart is shown in figure 5.

After an initialization process, the software starts with a scanning algorithm (pointing). As soon as there is power, sent from the communication partner, detected on the 4QD (acquisition), the scanning algorithm is interrupted and the software switches to the precise alignment of the communication partners (tracking). In case the signal from the communication partner is lost, the program goes back to the scanning algorithm (pointing), starting from the position of the last contact.

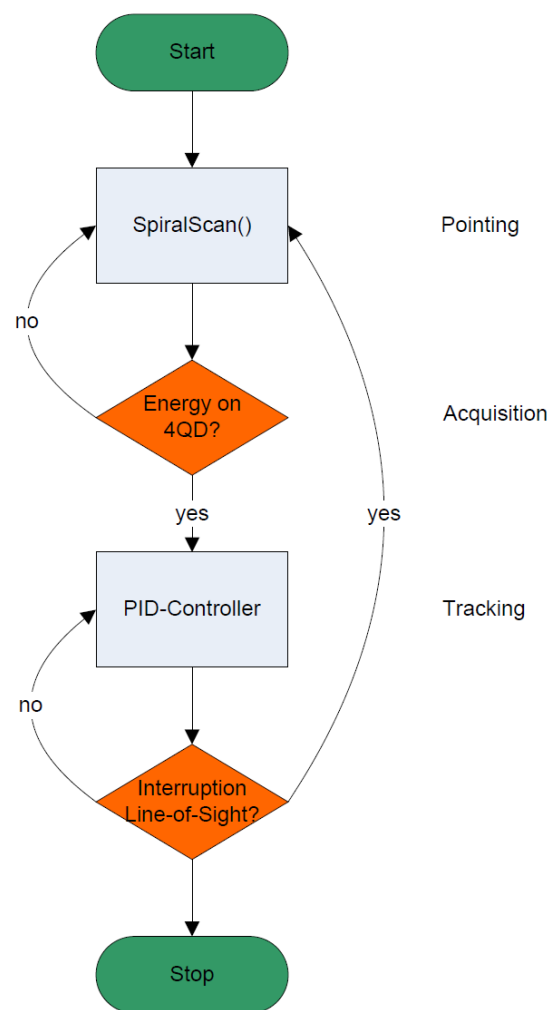


Figure 5: Blockdiagram of control software of PAT-system [4]

The aim of the scanning algorithm is an efficient and fast scan of the whole FoR of the SLT. This means, that the complete FoR must be scanned with no or minimal overlap.

Besides that, the momentum for the FSM must be limited to avoid damages at high speeds. With these conditions, a spiral pattern is applicable.

Two different kinds of spirals have been considered: the Archimedean spiral and the logarithmic spiral. Both types are shown in figures 6 and 7.

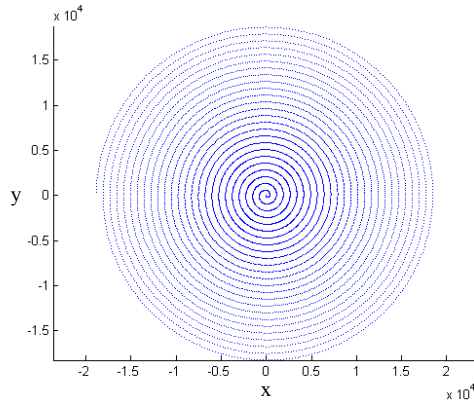


Figure 6: Archimedean spiral (MATLAB simulation) [4]

In Cartesian coordinates, a spiral is defined as:

$$x(\varphi) = r(\varphi) \cdot \cos(\varphi) \quad (1)$$

$$y(\varphi) = r(\varphi) \cdot \sin(\varphi) \quad (2)$$

with $r(\varphi)$ being the radius of the spiral depending on the angle of the arc φ .

For the Archimedean spiral, $r(\varphi)$ is defined as:

$$r(\varphi) = a \cdot \varphi \quad (3)$$

with a constant scaling factor a and angle φ . For the logarithmic spiral, the radius $r(\varphi)$ is defined as:

$$r(\varphi) = a \cdot e^{j \cdot \varphi} \quad (4)$$

with scaling factor a and gradient j [6].

The kind of used spiral depends on the acquisition scenario. The Archimedean spiral provides an equidistant scan of the FoR whereas the logarithmic spiral provides a more accurate scan in the center with increasing gradient in between the turns closer to the outer border of the spiral.

For the SLT, the Archimedean spiral has been chosen, because there is no knowledge about the position of the communication partner, so that the whole FoR must be scanned with the same resolution. To make sure that no communication

partner is missed, the distance between two turns must be at most the FoV of the 4QD. That means, the design of the optical system defines the FoV of the 4QD and thereby also the gradient of the spiral.

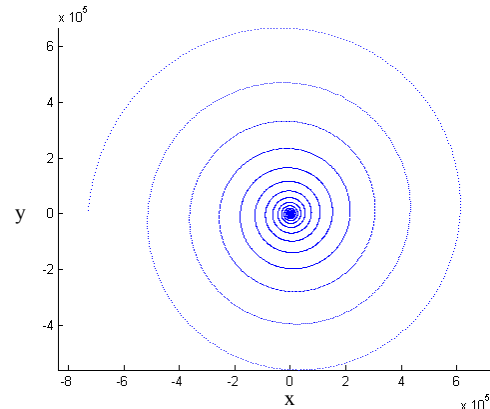


Figure 7: Logarithmic spiral (MATLAB simulation) [4]

The spiral starts in the center with an increasing radius until it reaches the outer border of the FoR of the laser terminal. To minimize the momentum for the FSM, the spiral goes on with the same direction of rotation but with a decreasing radius. Therefore, a mathematical description is needed to get a smooth change from increasing to decreasing radius without changing the direction of rotation. The behavior of the Archimedean spiral in time domain chosen for the SLT is shown in figure 8.

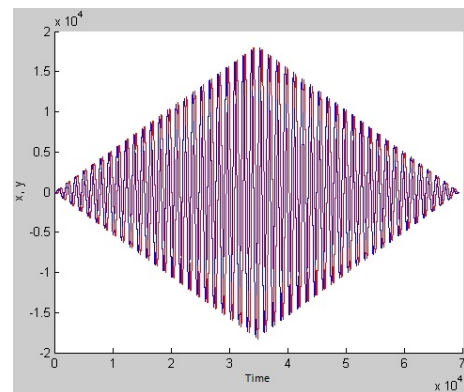


Figure 8: X and y (red and blue) coordinates of an Archimedean spiral in time domain (MATLAB simulation) [4]

Figure 8 shows the increasing radius of the spiral and the smooth change to decreasing radius. This process is repeated until a communication partner is acquired.

After acquisition, the software changes to the tracking mode. The aim of the tracking mode is to keep both communication partners precisely aligned. Therefore, a control loop consisting of a DSP and a 4QD is used. Due to a highly dynamic scenario with MAVs, a fast and precise control algorithm is needed. Thus, the control loop itself is

implemented as a PID-controller in the DSP-software. The block diagram of the implemented controller in interaction with the 4QD and the FSM is shown in Figure 9.

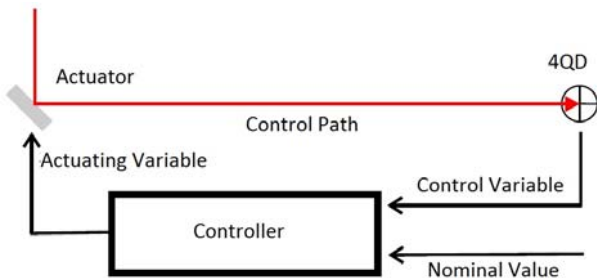


Figure 9: PID-controller implemented in DSP-software for tracking [4]

The 4QD is used as the feedback sensor for the PID-controller. The two control signals of the sensor are derived from the following relation:

$$X = (B+C) - (A+D) / (A+B+C+D) \quad (5)$$

$$Y = (A+B) - (C+D) / (A+B+C+D) \quad (6)$$

with the signals of the quadrants A, B, C and D (compare to figure 10) and the two axis X and Y of the FSM.

Figure 10 shows two typical situations in tracking mode: a perfect centrally aligned spot (left) and a spot out of alignment (right).



Figure 10: Spot position on the 4QD. Left: spot in the center - no PID-controller adjustment of FSM needed. Right: spot outside center - PID-controller adjustment of FSM needed [7]

In the left situation, all quadrants are equally lighted, so that X and Y equal zero, what means that there is no correction of the FSM position needed. In the right case, X and Y are unequal zero, so that the control software including the PID-controller has to correct the position of the FSM to get the spot centrally aligned [7].

V. MEASUREMENT

A prototype of the SLT has been set up in the laboratory at German Aerospace Center (DLR). The components of the terminal have a weight of 1.15 kg, a size of 18 x 28 x 6 cm and a power consumption of less than 11 W. The tests of the PAT-system lead to the following figures 11, 12, 13 and 14.

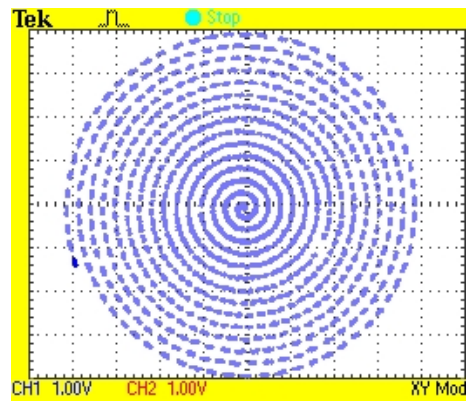


Figure 11: archimedean spiral scan pattern in XY-representation on oscilloscope [4]

Figure 11 shows the Archimedean spiral in XY-representation on the oscilloscope. It shows the same behavior as expected from the simulations shown in figure 6. Figure 12 shows the same spiral in time domain and fulfills the expectations from the simulation (compare figure 8). The measurement of the outer border of the spiral leads to an angle of +/- 23° from the optical axis, that means a FoR of 46°. In these measurements, the FSM is not running at maximum speed. At maximum speed, a complete scan cycle time (spiral from center to outer border) of less than 1 second can be reached.

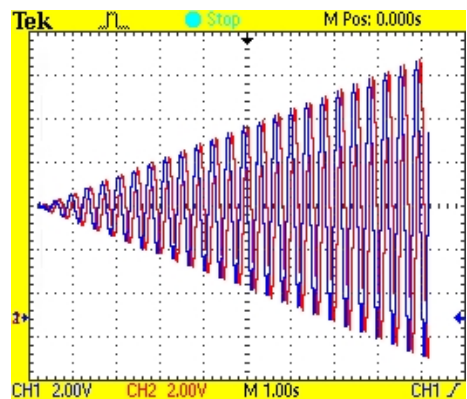


Figure 12: spiral scan pattern in time domain on oscilloscope [4]

Figure 13 shows the whole process of pointing, acquisition and tracking. After being switched on, the DSP software starts with the scanning process in the Archimedean spiral pattern (signals of x- and y-axis of FSM in red and blue, compare figure 12). After the spiral reached the outer border of the FoR the radius decreases. At (1) (acquisition), there is power detected on the 4QD (two of four channels of the 4QD in green and magenta), so the communication partner has been acquired. The software goes from pointing mode to tracking mode. The values for x- and y-axis of the FSM are calculated so that the values of the 4QD are equal what means that the spot is exactly aligned to the center of the 4QD (2) and the data receiver. Between (2) and (3) is no change in the spot position on the 4QD, so it is still centrally aligned and no movement of the

FSM is required. At (3) the connection has been interrupted by an obstacle in between the communication partners – the software jumps back to the scanning algorithm until the partner is acquired again (4). The values for x- and y- axis of the FSM are controlled by the PID-controller again to align the spot in the center of the 4QD (5). After a phase of no movement (5 to 6) there is a relative movement (6) between the communication partners so that the signal on the 4QD changes and the PID-controller adjusts the position of the FSM to compensate the movement and keep the communication partners aligned. At (7) the communication ends.

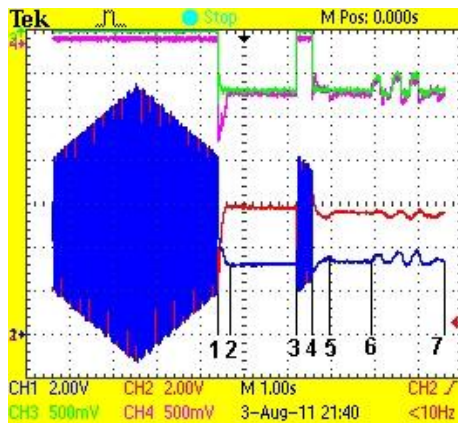


Figure 13: Behavior of PAT-system in time domain on the oscilloscope [4]

Figure 14 shows the movement of the FSM in XY-representation during tracking mode. For this measurement, the acquired communication partner performs a random movement that is detected by the 4QD. The PID-controller in the DSP calculates the displayed signal for x- and y-axis to compensate this movement.

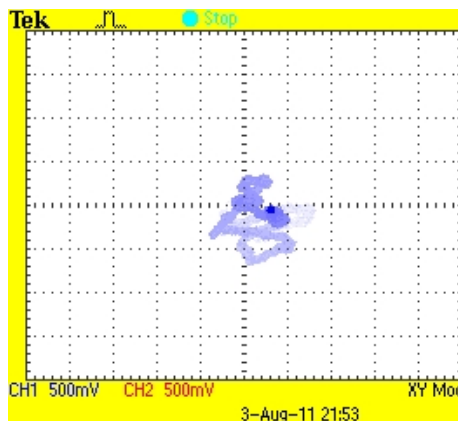


Figure 14: movement of the tip-tilt-mirror during tracking with moving communication partner (highlighted track) [4]

VI. RESULTS

The laboratory prototype of the SLT proves, that a small and lightweight laser terminal with a large FoR and a single actuator is possible. The terminal provides a FoR of 46° with a scanning cycle time of less than 1 second. The size of the terminal is $18 \times 28 \times 6$ cm at a weight of 1.15 kg and a power consumption of less than 11 W.

VII. OUTLOOK

With the development of the SLT a first step towards small and lightweight terminals is done. The goal for future developments is an overall system weight of less than 1 kg and a full hemispheric FoR at same resolution and scanning time.

VIII. BIBLIOGRAPHY

- [1] B. Epple, "Development and Implementation of a Pointing, Acquisition and Tracking System for Optical Free-Space Communication Systems in High Altitude Platforms", Diplomarbeit, Institut für Informatik, Ludwig-Maximilians-Universität München, http://www.pms.ifi.lmu.de/publikationen/diplomarbeiten/Bernhard.Epple/DA_Bernhard.Epple.pdf, 2005
- [2] C. Fuchs, J. Horwath, "Aircraft to ground unidirectional laser-communication terminal for high resolution sensors", German Aerospace Center (DLR), Institute for Communication and Navigation, Weßling, Germany, 2009
- [3] M. Knapek, F. Moll, J. Horwath, N. Perlot, "Experimental verification of optical backhaul links for high-altitude platform networks: Atmospheric turbulence and downlink availability", In International Journal of Satellite Communications and Networking, German Aerospace Center (DLR), Institute for Communication and Navigation, Weßling, Germany, 2007
- [4] C. Schmidt, "Optimiertes Strahlusrichtesystem für die optische Freiraumkommunikation", Diplomarbeit, Friedrich-Alexander-Universität Erlangen-Nürnberg Technische Fakultät, 2011
- [5] GRINTECH GmbH, "GRIN Objective Lenses for Endoscopy", Gradient Index Optics Technology (GRINTECH), http://www.grintech.de/downloads-12.html?file=tl_files/content/downloads/GRIN_Objective_Lenses.pdf, 2011
- [6] M. Löber, "Spiralen", Facharbeit im Leitungskurs Mathematik, http://www.phynet.de/schulklausuren/upload/Ma-Facharbeit_Spiralen.pdf
- [7] C. Fuchs, "Fine Tracking System for Aeronautical FSO Links", http://elib.dlr.de/60550/1/Fine_Tracking_System_for_aeronautical_applications_-_latest_submission_-_Ka_%26_Broadband_2009.pdf, German Aerospace Center (DLR), Weßling, Germany, 2009
- [8] J. Horwath, N. Perlot, M. Knapek, F. Moll, "Experimental verification of optical backhaul links for high altitude platform networks: Atmospheric turbulence and downlink availability", Int. J. Satell. Commun. Network., 25, 501-528, 2007